Regular Article – Atomic and Molecular Collisions

Cross sections and transport coefficients for electrons in C$_2$H$_6$O and its mixtures with Ar and Ne

Zoran Lj Petrović[1,2,a] , Olivera Šašić[3], Snježana Dupljanin[4], and Paul Maguire[2]

[1] Serbian Academy for Sciences and Arts, Knez Mihailova 35, 11000 Belgrade, Serbia
[2] School of Engineering, Ulster University, Jordanstown, Co., Antrim BT37 0QB, UK
[3] The Faculty for Traffic and Transport Engineering, University of Belgrade, Vojvode Stepe 305, 11000 Belgrade, Serbia
[4] Faculty of Natural Sciences and Mathematics, University of Banja Luka, Bosnia and Herzegovina, M. Stojanovića 2, 78000 Banja Luka, Bosnia and Herzegovina

© The Author(s) 2022

Abstract In this paper, we show and discuss a set of cross sections for electron collisions with dimethyl ether (DME, C$_2$H$_6$O) obtained by the standard swarm analysis of experimental data for drift velocities and ionization coefficients measured in pure DME and its mixtures with Ar and Ne by E. Oettinger and coworkers. While the existing cross section set gave relatively good predictions for drift velocities, it proved necessary to modify the inelastic cross sections in order to achieve a better agreement with drift velocities in gas mixtures and a good agreement for the ionization coefficient. Furthermore, the derived set of cross sections was used to calculate the electron transport and rate coefficients under the influence of a constant electric field and crossed electric and magnetic DC and RF orthogonal configuration fields. The effect of the magnitude and frequency of the fields on electron transport was studied separately. Our work has resulted in a database of collision and transport data which can be used in modeling of both DC and RF discharges and plasma applications containing pure DME and its mixtures.

1 Introduction

Dimethyl ether (DME) is one of the largest organic molecules in the interstellar space and its concentration in the star-forming regions may be significant [1]. This gas is an organic molecule that has extensive applications in the industry, transportation and high energy particle research. DME can be produced by dehydration of methanol, as well as by the extraction from jatropha seeds [2]. Because of its insignificant impact on environment and high cetane number (55), it is used as an alternative fuel for diesel engines [2, 3]. DME is also used in particle detectors, primarily in Micro Strip Gas Chambers [4–6], Gas Electron Multiplier (GEM) detectors [7], as well as in Liquid Cristal Polymer GEM detectors developed by Takeuchu and coworkers [8, 9], as an enhanced version of the previous detectors designed for satellite missions. Further advancement of such detectors, breakdown of the fuel mixtures or removal of the molecules potentially emitted into the atmosphere, requires knowledge of reliable electron transport and collisional data. In particular, such data would be of help in selecting the composition of the gas mixtures required for optimal operation

of particle detectors, through detailed models of discharges in DME.

As to our knowledge, there are only few experimental studies of electron transport properties in DME and only one available set of scattering cross sections. Bradbery–Nielsen technique was used in electron drift velocity measurements performed by Cottrell and Walker [10] and F. Villa [11]. Cindro and coworkers measured drift velocity in pure gas as well as in its mixtures with He [12], while Oettinger and coworkers measured drift velocity in pure gas and DME/Ar and DME/Ne mixtures [13]. Townsend ionization coefficient was measured by Cottrell and Walker [14], Sharma and Sauli [15] in pure DME and by Oettinger and coworkers in pure DME, as well as in DME/Ar and DME/Ne mixtures [13]. The only available set of effective cross sections for e^-/DME scattering was developed by S. Biagi and imbedded into the Magboltz code [16] (source file for version 10.0.2) which makes these data difficult to access. Also, as procedure and sources used to obtain these cross sections have not been fully presented, it is only clear that those cross sections have been derived by some form of swarm analysis, but the origins of the initial cross sections and the used transport data are not available to the users. In particular, it is uncertain whether ionization coefficients have been used to establish higher energy range of the cross sections (for practical purposes from 5 to 30 eV).

[a] e-mails: z.petrovic@ulster.ac.uk;
zoran@ipb.ac.rs (corresponding author)

Having in mind the importance of the data for this molecule for a number of gases used in elementary particle detectors, the present work is our attempt to overcome this discernible deficiency of the reliable and well-documented data.

First, we performed a standard swarm analysis on the set of experimental results [13] that seemed to be the best available, in order to obtain a consistent and complete set of cross sections. Furthermore, we proceeded to analyze electron kinetics in cases when constant and time-varying electric and magnetic fields were applied in order to check what kind of kinetic phenomena may be expected to occur [17, 18].

2 Swarm procedure and the input data

A detailed description of the swarm procedure has been given earlier in a number of publications [17, 19–22], and its advantages and limitations have also been discussed in great detail elsewhere [17]. Briefly, the starting set of cross sections is used as an input into the iterative process of transport parameter (drift velocity, ionization coefficient, characteristic energy, etc.) calculations. In each of the numerous steps, cross sections are modified in order to achieve the best possible level of agreement between measured and calculated sets of transport data. Even small alterations in the total momentum transfer cross section may cause dramatic changes of the drift velocity. At the same time, ionization coefficient is most sensitive to processes that have thresholds close but below the threshold for ionization [18]. Because of that the process of cross section modification is performed step by step within very narrow energy intervals defined by the range of the experimental transport data. Having said that we also need to extrapolate cross sections well beyond that range in order to achieve functioning calculations but outside the well covered initial mean electron energy range the sensitivity to the cross sections is significantly reduced. In this paper, the starting set of cross sections is that of Biagi [16]. The experimental transport data are taken from E. Oettinger and coworkers [13]. The limiting factor in achieving a high degree of uniqueness of derived cross sections is the small number of different transport coefficients and the limited energy range. This problem can be mitigated by including binary mixture measurements of transport coefficients in the procedure. That is why we used results for 20% and 50% of DME in Ar and 50% of DME in Ne [13] and fitted our calculations to all of those results simultaneously. For e/Ar and e/Ne scattering, we used the cross section sets of Hayashi [23] and Morgan [24], respectively. Those sets were based in particular on the most accurately determined cross sections for electrons in rare gases determined by Robert Crompton and coworkers [20].

We used two computer codes to calculate transport coefficients: Elendif [25] and our well-tested Monte Carlo (MC) simulation code [26]. All definitions of transport coefficients were given in our previous publications [26]. The first code is based on solving the Boltzmann equation in two-term approximation (TTA). Bearing in mind all approximations and limitations regarding the accuracy of the TTA calculation method and its applicability, which were reasonably questioned on many occasions [27], this code nevertheless fulfills our requirements regarding efficiency. It provides a large number of calculated points rapidly, and consequently, it was used for repeated iterations. Final results from the two-term code have served us as a set for the Monte Carlo code. Final results were obtained by the MC code. In the MC simulations, the motion of a large number of charged particles (in our case electrons) through a neutral (not ionized) background gas under the influence of electric field (or electric and magnetic) is followed. We have also observed the evolution of the electron swarm under the influence of spatially uniform and time independent as well as time-varying crossed electric and magnetic fields, with the phase shift of $\pi/2$. An electron swarm was released from the origin with the mean energy of 1 eV and the initial distribution function was assumed to be a Maxwellian. The initial number of released electrons varied from $2.5 \cdot 10^5$ to $5 \cdot 10^5$. Electronic scattering was considered to be isotropic, and it was represented by a set of effective cross sections as an input. The input data also included the gas concentration which was taken to be $3.54 \cdot 10^{22}$ m^{-3}, at the temperature of 273 K, corresponding to the gas pressure of 1 Torr (1 Torr = 133.322 Pa). All calculations, for the case when DC electric fields were applied, were performed over a broad range of reduced electric fields (E/N), from 1 Td, up to 1000 Td (1 Td = $1 \cdot 10^{-21}$ Vm^2) covering mean energies from the thermal energy at 293 K up to 10 eV.

In the case of constant $E \times B$ fields, electric field took values from 1 Td up to 2000 Td, while the reduced magnetic fields were B/N = 100 Hx, 200 Hx, 500 Hx, 1000 Hx and 2000 Hx (1 Hx = 10^{-27} Tm^3). In order to study the influence of the magnitude of reduced magnetic field in cases when time-varying (RF) fields were applied, we calculated transport coefficients for E/N = 100 Td, B/N = 0 Hx, 100 Hx, 200 Hx, 500 Hx, 1000 Hx, and 2000 Hx, while frequency of the fields was 100 MHz. Later on, our focus was on the effect of field frequencies on transport properties, so the E/N was 100 Td, B/N = 0 Hx and 1000 Hx, while frequencies were 10 MHz, 50 MHz, 100 MHz, 500 MHz and 1000 MHz. All transport and rate coefficients were calculated in case of pure DME, and mixtures with Ar and Ne. However, in this paper, only few of the results are presented, that is for pure gas in case of constant crossed fields, and for 20% DME/Ar mixture in case of RF fields.
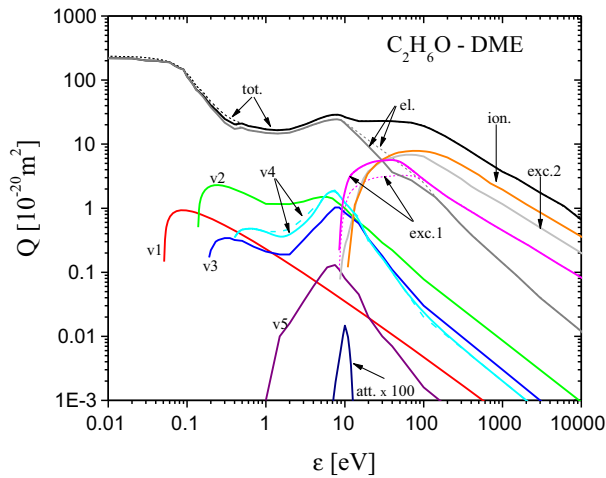
Fig. 1 The final, swarm derived set of cross sections for e-/DME interaction (solid lines): total and elastic momentum transfer (tot, el), vibrational excitations (v1, v2, v3, v4 and v5) dissociative excitations (exc1 and exc2), electron attachment (att × 100) which is multiplied by 100 for the reasons of visibility, and the ionization cross section (ion.). Dashed lines represent the initial cross sections of S Biagi [16]

3 Results and discussion

3.1 Cross section set for e⁻/DME interactions and transport coefficients in DC electric field

The ultimate result of this work is the complete set of cross sections for electron collisions with DME molecules, obtained by the swarm procedure. Figure 1 presents that set and henceforth we shall refer to it as the final set.

The starting cross sections of Biagi (dotted curves in Fig. 1) were modified in order to get the best possible fit of calculated values for drift velocities (W) and ionization coefficients (α/N) to experimental results, for pure gas and for 20% and 50% DME/Ar and 50% DME/Ne mixtures, simultaneously. Figures 2–6 show comparison between the data obtained with the initial cross sections and the final set, as well as with other sources of data available from the literature. Note that, in most cases, the initial calculations are made with the two-term code, while the final results are always obtained both with the two-term and MC code.

As it can be seen from Fig. 2, a fairly good fit to experimental results of the drift velocity in pure gas can be obtained when calculations are made even with the initial set of cross sections. In the mixture with a noble gas, where the abundance of the molecular gas is reduced, the departure of calculated data from the measurements becomes discernible (see Figs. 3 and 4). There is a combination of at least two circumstances which resulted in the occurrence of such differences. Most importantly, inelastic processes in the molecular gas will change mean energy of the swarm, and thus, the effective momentum transfer would change especially
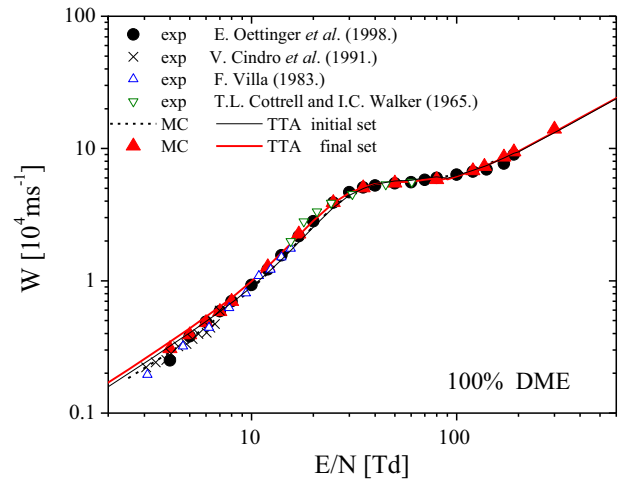

Fig. 2 Drift velocity for electrons in pure DME as a function of E/N: comparison between present results (solid line, solid triangle), results obtained with the starting cross sections (open circles) and previously published experimental data
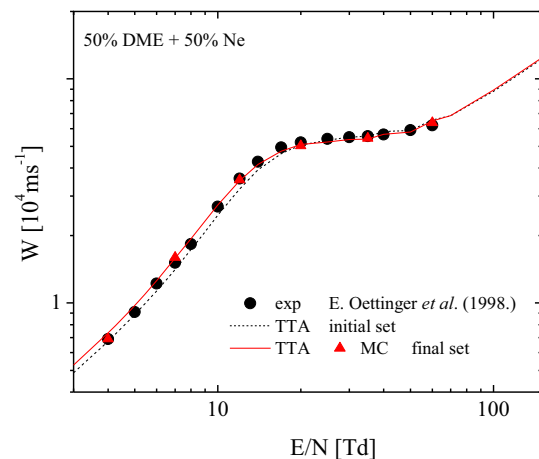

Fig. 3 Drift velocity for 50% DME/Ne mixture as a function of E/N

in gases with a strong energy dependence of the elastic/momentum transfer cross sections. Consequently, it appears that although the number and the momentum balances are satisfied, the energy balance has yet to be achieved by inelastic cross section adjustments (This claim becomes more evident from the ionization coefficient calculations for the pure gas and 50% mixture with Ar, that are presented in Figs. 5 and 6, respectively). The impact of inelastic processes is evident in the mixture data in Ar due to the occurrence of negative differential conductivity (NDC).

Second, applicability of the two-term approximation may be questionable even in the low electron energy region, due to the existence of pronounced vibration excitation cross sections and the energy-wise concurrent steep slope in the momentum transfer cross section.
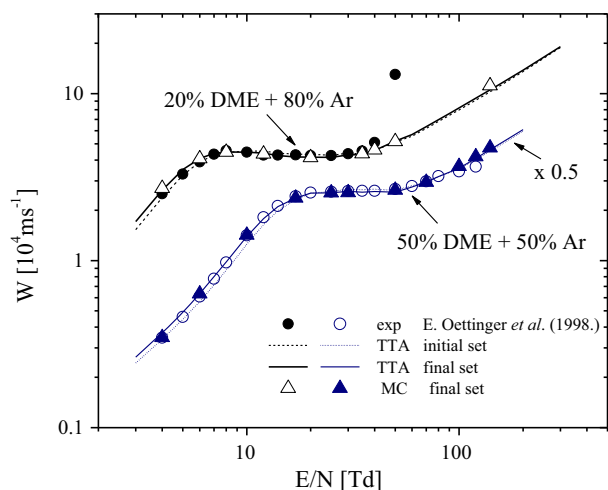
Fig. 4 Drift velocity for electrons in 20% and 50% DME/Ar mixtures as a function of E/N. Results for 50% mixture are multiplied by the factor of 0.5 for better readability of the graph
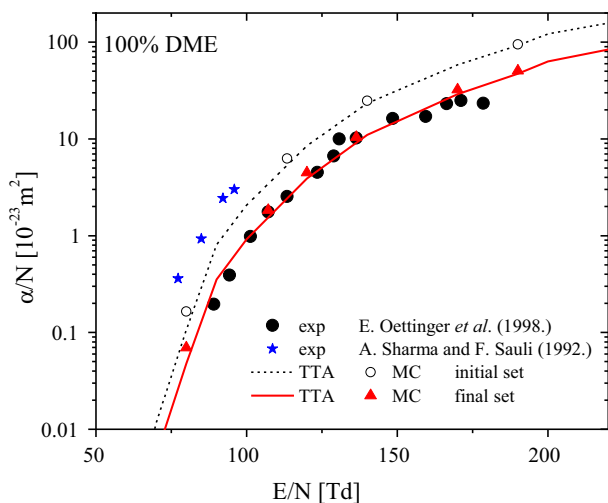

Fig. 5 Ionization coefficient in pure gas as a function of E/N: comparison of experimental data with the calculations obtained with the initial set of cross sections (dashed line, open circles) and the final (recommended) set of cross sections (solid line, solid triangles)

It turned out that E/N dependencies of the drift velocity below $E/N = 20$ Td were mostly sensitive to inelastic cross section modifications around 2 eV. As a result, the magnitude of the vibration excitation with the energy threshold of 0.349 eV (labeled as v4 in Fig. 1) was decreased by 25% in the energy interval between 1.5 eV and 4 eV. At the same time, total momentum transfer cross section had to be slightly decreased for the lowest energies below 0.4 eV. That reduction in the magnitude was not higher than 14%.

In Figs. 5 and 6, we show values of the ionization coefficients both calculated and measured and also both for the pure gas and for the gas mixtures with Ar and Ne. A
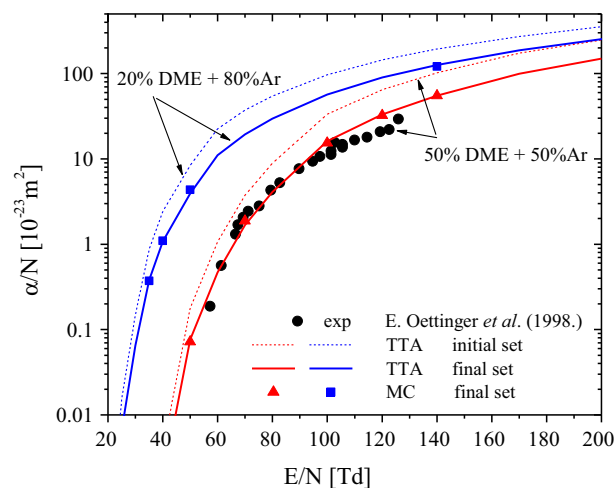

Fig. 6 Ionization coefficient as a function of E/N in 20% and 50% DME/Ar mixture: comparison between experimental and calculated data. Calculations are made with the initial set of cross sections (dashed lines) and the final set (solid triangles and squares)

large difference between the results based on the initial set and on the final set reveals the need for this analysis and also indicates that inelastic energy losses have not been properly accounted for in the initial analysis. In principle, most of the swarm studies were focused onto the low energies [20] because it was possible to reduce the number of active inelastic processes and especially in rare gases to reach the values of the momentum transfer (elastic) cross section that is unique and very accurate (in that respect data for He are the benchmark that has not been surpassed by other techniques). Nevertheless, applications dictated the need to cover higher energies (where standard swarm experiments do not work very well) especially the range of mean energies from 2 to 10 eV or more. This is dictated by the need to have sufficient ionization to sustain the relevant gas discharges. To cover the range of energies required for modeling of gas discharge lasers, Phelps has devised a procedure that consisted of the standard swarm procedure for the low energies but augmented by combined measurement of excitation coefficients for various transitions and also measurements of ionization coefficients [28, 29]. Due to a limited number of gases covered by such measurements and difficulties in establishing absolute emission calibration, Petrović and coworkers have developed an alternative technique that would take advantage of the readily available measured ionization coefficients from the pulsed Townsend (PT) technique [30]. There, one would perform low energy swarm analysis based on the existing low energy data, and then, for the energies relevant for gas discharges, one would take the PT data and make analysis for drift velocities together with the calculations of the ionization coefficients. In that procedure, it is assumed that the available data for excitation cross sections are accurate and most importantly that the measured ionization cross sections are known to a sufficiently high accuracy to be

accepted 'as is.' In that case, all the modifications would be made on the least well-known cross section that is usually dissociation to the neutral state. Thus obtained cross section after modification (through fitting of the ionization coefficients) would also carry with itself all the effects due to processes that were not included, as well as the inaccuracies in other excitation and ionization cross sections. It is important that the energy loss is high enough so that it may affect strongly the electron energy distribution function (EEDF) at higher energies than its threshold and that its energy profile is not energy selective (i.e., is broad akin to the cross sections for the singlet states).

As the values of ionization coefficients calculated from the initial set of cross sections were systematically higher than the measured ones (see Figs. 5, 6), the excitation cross section with the energy threshold of 7.7 eV (labeled as exc1 at Fig. 1) had to be increased in order to reduce the number of electrons in the high energy tail of the distribution function. The alterations were made in the energy region between 8.5 eV and 80 eV and the rescaling of the cross Sect. (7.7 eV threshold) was made step by step by multiplying with an energy dependent factor that varied in the interval from 1.1 up to 2.

The final elastic momentum transfer cross section was obtained when the sum of all inelastic processes was subtracted from the total momentum transfer. As a result of all cross section adjustments that we have made, elastic momentum transfer differs from the starting one over three energy intervals. It is reduced up to 16% between 0.004 and 0.4 eV, increased by less than 1% between 1.4 and 4 eV, while its magnitude is reduced from 0.16% up to 70% between 8 and 140 eV.

Our analysis shows that all cross section modifications that lead to the final set improved the agreement between measurements and calculations so the experimental results could be reproduced within the experimental uncertainties. This statement is true in all cases except for the last point for drift velocity in 20% DME/Ar mixture (see Fig. 4). No matter what we did with the cross sections, the departure of that point from our calculations could not be reduced without spoiling the agreement of other results. So, we conclude that some error must have occurred in presenting the results of measurements or that experimental uncertainty at the boundaries exceeds that for the standard covered range. In addition, good test for the accuracy of our results is the occurrence of the negative differential conductivity (NDC) in E/N dependence of the drift velocity for 20% DME/Ar mixture in the region from 10 Td up to 25 Td (See Fig. 4) that we were able to reproduce quite accurately. The same, but indistinct phenomenon occurs for the pure gas in the interval from 80 Td up to 90 Td. This kinetic (transport) phenomenon is not readily noticeable and that fact can be explained by a large momentum transfer cross section in comparison with the inelastic cross sections in the corresponding energy region. More prominent NDC could be expected in the mixtures with Ar where DME is present in smaller abundances.
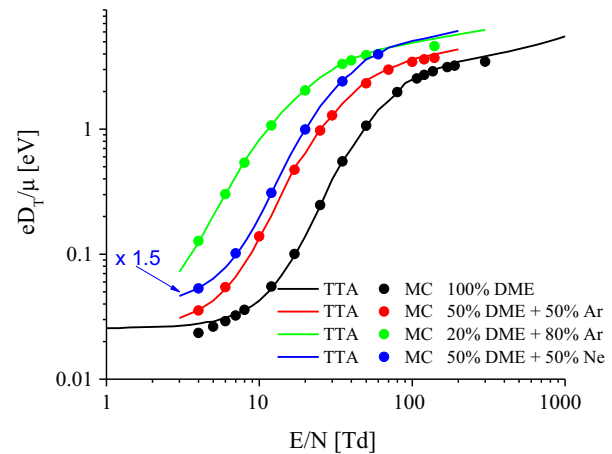

Fig. 7 Characteristic energy as a function of E/N for pure gas and mixtures. Note that, the data for 50% DME/Ne mixture are multiplied by 1.5 for the reason of visibility

Minor discrepancies for the ionization coefficient at the highest E/N and for the drift velocities at the lowest E/N could indicate a need to improve the cross sections further or simply the increased uncertainties close to the edge of the applicability of the experimental technique. In order to resolve such discrepancies, one should have accurate measurements of vibrational and electronic excitation coefficients, or a more reliable ionization cross section, at least.

Finally, we used the final set of cross sections in order to calculate other transport parameters, such as characteristic energies and rate coefficients for individual inelastic processes for both pure gas and mixtures for a constant electric field. We will present here characteristic energies for pure gas and mixtures (Fig. 7). As expected, the energy (E/N) dependencies of characteristic energies may be explained by the predominance of different inelastic processes described through their cross sections. Even though characteristic energies have not been measured for DME and its mixtures, it is in principle possible. Characteristic energy is thus used to fix the inelastic cross sections. These data may also be used to provide diffusion coefficients for fluid modeling in DME and DME containing mixtures. Characteristic energy closely resembles mean electron energy (with a numerical factor that is often 3/2 but not in the entire E/N range). Mean electron energies may not be measured by the known techniques but are readily calculated (mean energies for electric field only in pure DME may be seen for the magnetic field of 0 Hx in Fig. 8 where we show data for crossed electric and magnetic fields). PT technique often produced longitudinal diffusion coefficient or renormalized the longitudinal characteristic energy. This parameter is however not so sensitive on inelastic processes and is more often expanding on the information obtained from the drift velocities on momentum transfer. Most importantly when experiment focuses on drift velocity, accuracy of the thus obtained longitudinal diffusion coefficient is reduced
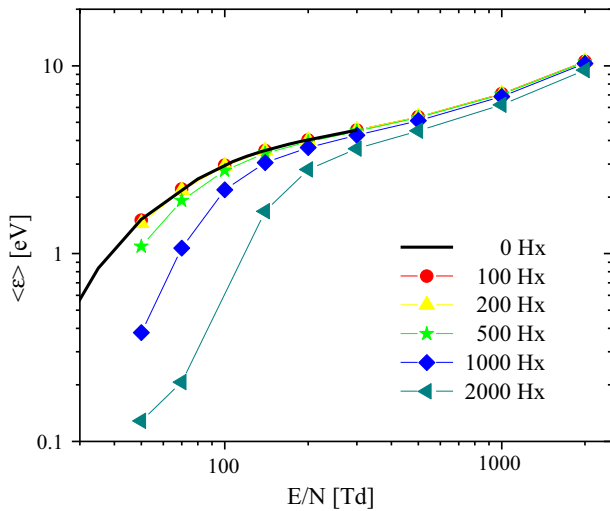
Fig. 8 Electron mean energy as a function of reduced electric field (E/N) for different reduced values of applied magnetic field (B/N) in pure DME

and these results are often not presented or used in the cross section analysis.

### 3.2 Transport of electrons in constant (DC) E × B fields

In the past few decades, the study of the transport characteristics of electron swarms in the presence of crossed electric and magnetic fields has increased significantly due to the high use of low-temperature plasmas that involve magnetic fields such as inductively coupled plasmas [31, 32]. Applications of these plasmas are wideranging from the magnetically confined gas lasers, high energy particle detectors to various plasma technologies incorporating magnetically enhanced plasma reactors. In this section, we present some results obtained by MC simulations of electron transport trough neutral DME under the influence of DC crossed electric and magnetic field with orthogonal configuration. We

have used the final set of cross sections for e-/DME scattering (Fig. 1). A detailed description of the procedures and mathematical relations for the calculation of the transport coefficients can be found in [26]. Under these conditions, new transport coefficients are generated, such as drift velocity and diffusion coefficient both in $E \times B$ direction, for example. For a more detailed description of these transport coefficients and accurate treatment of the effects associated with the magnetic field influence on electron transport, the reader should check some of earlier publications [7, 18, 33]

The basic parameter for describing electron transport in $E \times B$ fields is the ratio of the cyclotron and collision frequency (Ω/ν_c) [34, 35]. For all conditions covered here, this ratio was less than 1, so the transport was taking place in a regime that was dominated by collisions. As expected, the influence of the magnetic field on transport parameters becomes noticeable only for the highest values of B/N, and as the electron mean energy decreases with an increase in the magnetic field, the energy dependences of the other transport parameters resemble those for the case of no magnetic field, only shifted toward higher energies (see Fig. 8). The longitudinal component of the drift velocity does not appear to be affected significantly by a magnetic field of less than 1000 Hx (Fig. 9a). This is because the electron transport remains to be governed by collisions due to relatively large inelastic cross sections, even for high values of the magnetic field. On the other hand, perpendicular component of the drift velocity (Fig. 9b) increases dramatically with the magnetic field, as expected. The overall effect is shown in Fig. 9c. As it can be seen, the negative differential conductivity that occurs in the absence of the magnetic field (solid curve) cannot be observed when the magnetic field of at least 1000 Hx is applied. For lower B/N values, NDC exists at the corresponding energies, but it is inconspicuous.

As far as the energy dependences of the diffusion coefficients are concerned, there are two pronounced regions to be observed. The first is the region of rapid growth of the coefficients corresponding to a decreasing cross section for vibrational excitation and the minimum

Fig. 9 Drift velocity as a function of reduced electric field (E/N) for different values of reduced magnetic fields (B/N) in pure DME: longitudinal component (**a**), perpendicular component (**b**) and the total drift velocity obtained as $W = \sqrt{W_E^2 + W_{E \times B}^2}$
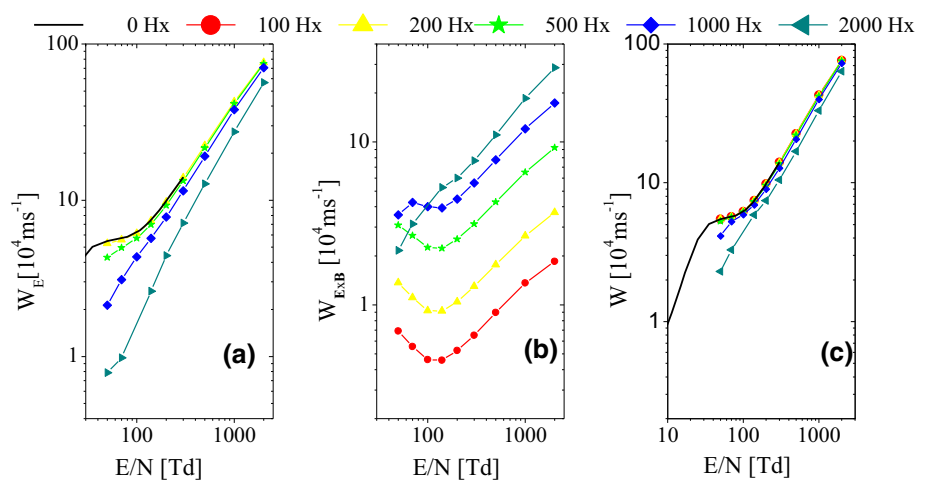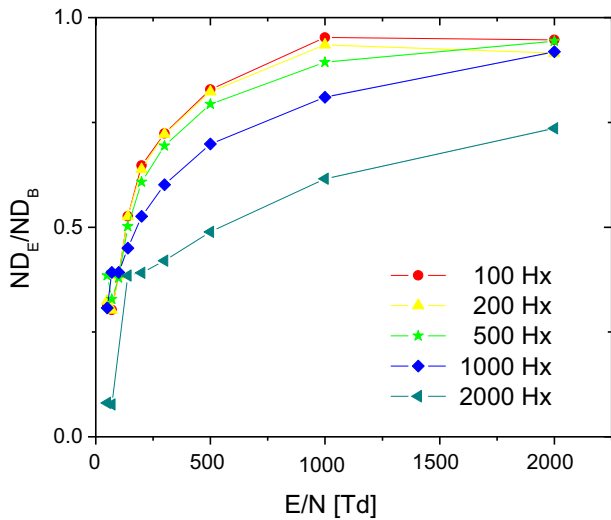
Fig. 10 The ratio of longitudinal and transverse component of diffusion coefficients as a function of reduced electric field (E/N) for different values of applied magnetic fields (B/N) in pure DME
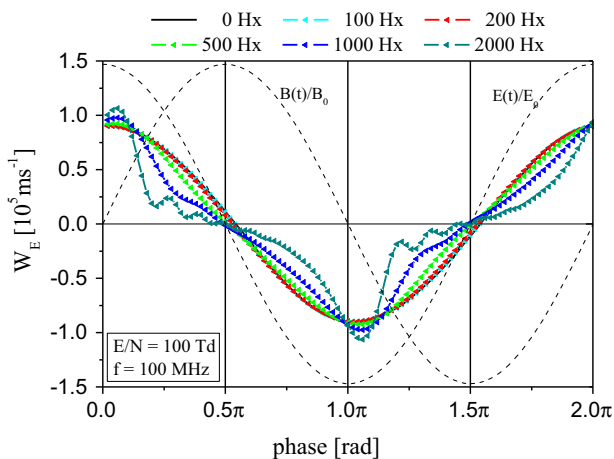

Fig. 11 Time dependence of the longitudinal drift velocity as a function of B/N. The frequency of the electric field is 100 MHz at $E/N = 100$ Td in 20%DME/Ar mixture

in the momentum transfer cross section. The second region is the slow growth of diffusion coefficients and it corresponds to the increasing inelastic cross sections for electronic excitation and ionization that impede the diffusion. However, this sensitivity of the diffusion coefficients is not sufficient to detect the finer structure of the energy dependence of the cross sections. In addition, one can see from Fig. 10 that the diffusion is anisotropic but only slightly, especially for strong electric fields, and low magnitudes of magnetic fields, as the ratio of longitudinal and transverse components of diffusion coefficients approaches 1.
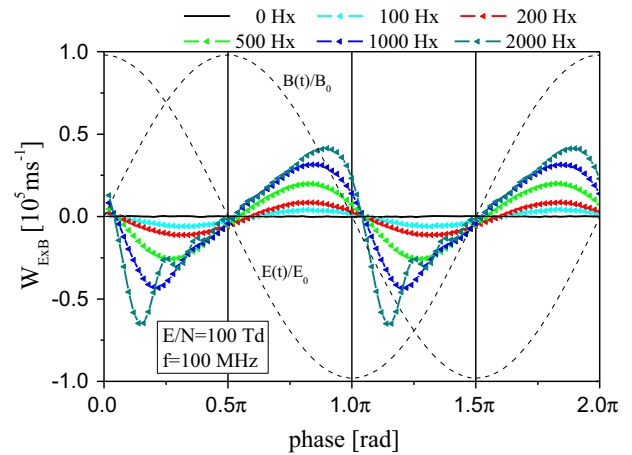

Fig. 12 Time dependence of the perpendicular component of the drift velocity as a function of B/N. The frequency of the electric field is 100 MHz at $E/N = 100$ Td in 20%DME/Ar mixture

3.3 Transport of electrons in time-varying (RF) E × B fields

In this section, we present results obtained by considering the transport of an electron swarm in a mixture of 20% DME + 80% Ar under the influence of the time-varying (RF) $E \times B$ fields with a $\pi/2$ phase difference between the two fields. Results for the mixtures provide more structure of the waveforms, and thus, this mixture was selected to present the data. We performed several series of calculations by using the MC code in order to obtain transport and rate coefficients as a function of E/N, B/N and frequency. In all cases, the given values of the fields refer to peak values. Similar calculations for other gases have produced a wide range of observations of interesting kinetic phenomena [18, 34]. In addition, most applications of the present day low-temperature plasmas occur in time-varying fields often sinusoidal. The ability of electrons to follow the external field is key to gaining energy required to sustain the plasma.

As it can be seen from Fig. 11, for B/N of less than 1000 Hx, magnetic field has almost no effect on the longitudinal component of the drift velocity. Some departure from the sinusoidal shape becomes visible only for the highest values of the magnetic field (1000 Hx and 2000 Hx). The shape becomes narrow and some slight oscillations, as a result of cyclotron motion, are observed. This shape and phase delay affect energy gain from the electric field by electrons.

The perpendicular component of the drift velocity (Fig. 12) increases with B/N and changes its shape from sinusoidal to a saw tooth profile. For the highest B/N, it is asymmetric, so mean value is not zero, and there are some visible oscillations too.

On this occasion, we shall not present results for temporal profiles of diffusion coefficients as a function of the magnetic field. Let us just confirm that all three coefficients behave as expected. Both longitudinal (ND_L) and diffusion in the $E \times B$ direction ($ND_{E \times B}$) are
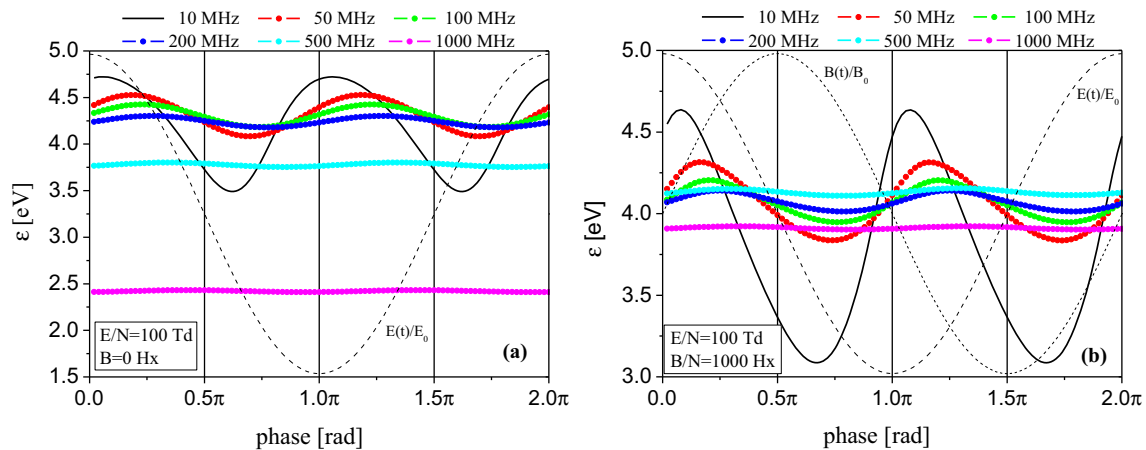
Fig. 13 Time dependence of the mean energy as a function of the frequency of the electric field: **a** $E/N = 100$ Td, $B/N = 0$ Hx; **b** $E/N = 100$ Td, $B/N = 1000$ Hx in 20%DME/Ar mixture

decreasing functions of B/N, highly modulated with the peaks shifted toward the part of the phase where the electric field goes through its maximum values. On the other hand, transverse diffusion coefficient (ND_B) is almost not affected at all by the magnetic field: Temporal profiles remain unmodulated and the reduction in the peak values is nearly imperceptible. Negative diffusion [36] was not observed presumably due to the collisional nature of the electron transport under present circumstances and energy dependences of the cross sections.

Figure 13 shows the time dependencies of the electron mean energy as a function of the field frequency for the case when (a) magnetic field is not present; (b) magnetic field is $B/N = 1000$ Hx. In both cases, we see a decrease in the mean energy as the frequency of the field increases. At the lowest frequency of 10 MHz, the mean energy profile is highly modulated, while at the highest frequency of 1000 MHz, the modulation disappears completely. In latter case, the temporal profile of the mean energy behaves as in an effective DC field. At higher frequencies (500 MHz and 1000 MHz), the decrease in the mean energy with increasing frequency of the field is more pronounced in the absence of the magnetic field.

In Fig. 14, we try to indicate the effect of the frequency on the longitudinal drift velocity in the absence of the magnetic field. As can be seen from Fig. 14, temporal profiles of the electron drift velocities maintain an almost sinusoidal profile for all frequencies of the applied field, with very broad peaks of nearly identical values. This is the result of a rather uneventful energy dependence of the momentum transfer cross section in pure DME (situation is expected to be quite different in Ar-DME mixtures with smaller abundances of the latter gas). However, there is a noticeable phase shift of the profiles, and mean values decrease with the increment of the frequency. Apparently, there is no sign of time resolved negative differential conductivity [37].

Figure 15 shows the time dependence of the drift velocity in the $E \times B$ direction, at $E/N = 100$ Td
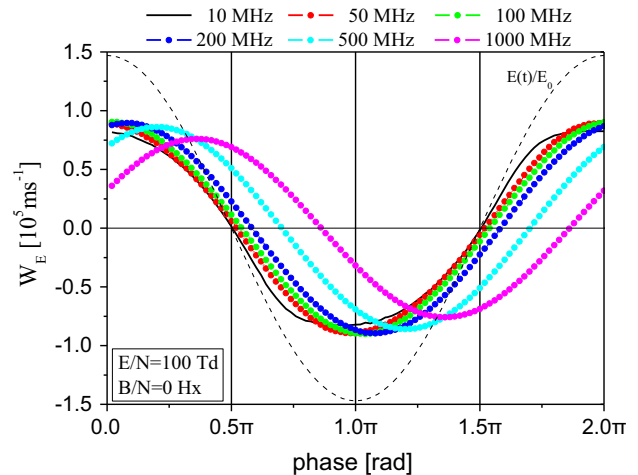

Fig. 14 Drift velocity of electrons in RF $E(t)$ field at different frequencies of the field for $E/N = 100$ Td in 20%DME/Ar mixture

and $B/N = 1000$ Hx, for different frequencies. At lower frequencies, the profile is extremely asymmetric and that asymmetry slowly disappears as frequency increases. At the same time, mean value of the drift velocity increases which results in macroscopic rotation of the electron swarm. For 1000 MHz, the drift velocity does not change direction at all. This has already been observed for other gases [38] but has not been documented well in the literature.

Figure 16 presents the temporal profiles of the longitudinal (ND_L) and transverse (ND_T) diffusion coefficients at $E/N = 100$ Td, $B/N = 0$ Hx and $f = 10$ MHz. From this figure, it is obvious that anomalous longitudinal diffusion occurs [35, 39, 40] for this gas. Briefly, the ND_L coefficient profile peaks during, or just after the part of the phase where the electric field goes through zero and changes its sign. There, it is expected that both diffusion coefficients would reduce to their thermal value. At the same time, for a brief period of
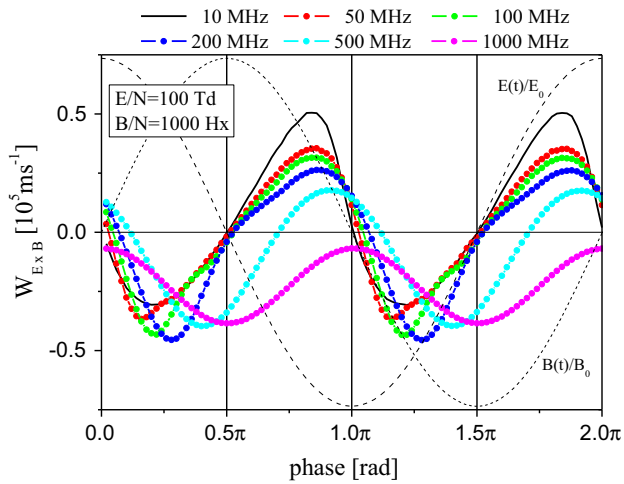
Fig. 15 Time dependence of the perpendicular component of the drift velocity as a function of the frequency of RF $E \times B$ field, at $E/N = 100$ Td, $B/N = 1000$ Hx in 20%DME/Ar mixture
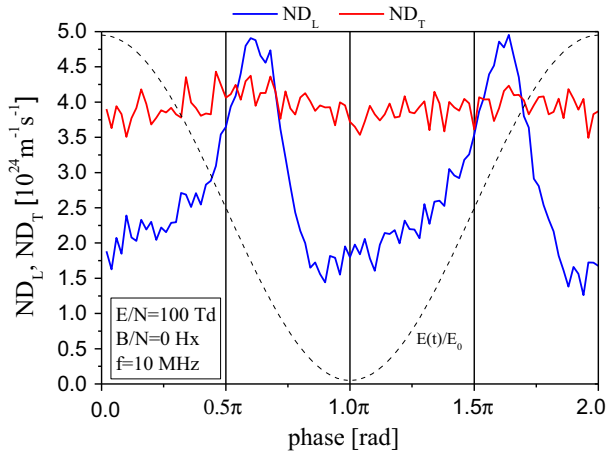

Fig. 16 Temporal profile of diffusion coefficient in case of time-varying electric field, $E/N = 100$ Td, $f = 100$ MHz in 20%DME/Ar mixture

phase (time), ND_L becomes unexpectedly larger than the ND_T. In case of DC fields, as we have already seen (Fig. 10), the situation is reversed: The diffusion is anisotropic and the ND_T coefficient remains larger than the ND_L for the same energy range. As frequency increases, this effect slowly decreases, as well as modulation of the temporal profiles, and at the frequency of 500 Hz, diffusion becomes slightly anisotropic and modulation disappears.

4 Conclusion

This paper presents our final results on the cross sections for electrons in DME and also it provides a broad discussion of the behavior of the transport coefficients in $E \times B$ DC and RF fields. Preliminary presentations of these results at conferences occurred over a period of 6 years [41–43]

Using a standard swarm procedure, with the starting cross section set of Biagi, a new set of complete cross section data for electron interaction with DME molecule is obtained. The input in the procedure was the set of experimental results for the drift velocity and the ionization coefficient, measured by E. Oettinger and coworkers, in case of pure gas, as well as in 20% and 50% mixtures with Ar and 50% mixture with Ne. The analysis was conducted simultaneously for pure gas and all mixtures. Two computer codes were used for the calculations: one that solves the Boltzmann equation in the two-term approximation, and the second one was a Monte Carlo code. As a result of the analysis, the total and the elastic momentum transfer cross sections, vibrational excitation ($\varepsilon_{th} = 0.349$ eV) and electronic excitation cross sections ($\varepsilon_{th} = 7.7$ eV) were modified. The derived set is consistent with all experimental results. In all cases, discrepancies between measured and calculated transport parameters are within the combined experimental and numerical uncertainties. For a further improvements of the cross sections, perhaps to the same degree of accuracy as in the case of other swarm derived cross sections (noble gases, for instance), new measurements are needed. In particular, additional studies of electronic and vibration excitations, as well as the measurements of characteristic energies, would be of great interest. Nevertheless, this set of cross sections should work well for modeling collisional plasmas and plasma applications containing pure DME and its mixtures with other gases. It will provide overall number, momentum and energy exchange rates although specification of specific channels may be difficult due to the inherent non-uniqueness of the swarm derived cross sections.

In accordance with the analysis of Casey et al. [44], we have shown only the bulk drift velocities in our plots. As for the difference between the two-term and multi-term/MC results [27], it has been represented as the difference between the lines and the corresponding points labeled MC. We are not in the range of excessive differences both between bulk and flux transport data and two-term and multi-term results.

In principle, our cross sections should be complete and thus provide a good overall exchange of the number, momentum and energy of the electron swarm. It appears that the initial set did not take advantage of the inelastic processes and thus our modification was required.

As a side result of our study, we obtained a set of transport (e.g., electron mean energy, drift velocity and diffusion coefficients) and rate coefficients for pure gas, as well as for mixtures, in case when constant electric field is applied. As expected, the energy dependencies of the transport parameters follow the trends defined by the cross sections. In pure gas and 20% DME/Ar mixture, negative differential conductivity occurs in narrow energy regions, that correspond to the fields of

E/N = (80–90) Td, and E/N = (10–25) Td, respectively. Our next goal was to provide a set of transport data in pure gas for the case when constant crossed electric and magnetic fields with orthogonal configurations are applied. Transport coefficients were calculated over a broad range of E/N and for five different values of B/N. Those conditions ensured that all calculations were made in the collision dominated regime. The cooling effect of the magnetic field was observed, as expected, as well as the fact that diffusion of electrons is anisotropic. Finally, we used the derived set of cross sections and our MC code in order to study the electron transport under time-varying electric and crossed electric and magnetic fields with the phase difference of $\pi/2$. In this paper, we present only the results for 20% DME/Ar mixture. The influence of the magnitude and the frequency of the fields on transport parameters were studied separately. Results showed that magnetic field strongly affects electron transport producing complex behavior of the corresponding coefficients. Interesting kinetic phenomena, such as the time resolved negative differential conductivity and negative diffusion, were not observed. However, anomalous longitudinal diffusion occurs in case of low field frequencies, and diffusion is slightly anisotropic. Our analysis suggests that the use of standard approximations, such as the effective field approximation and instantaneous field approximation, in plasma models is at least questionable [45].

The data for cross sections not only provide a basis for the expected applications such as modeling of elementary particle detectors [46–48] as well as the breakdown in alcohol based fuels. One may pay attention to another aspect of energy related issues, i.e., storage of excess energy from the sustainable energy sources. While most often production of CO from CO_2 is sought [49], one may also look for production of some alcohols or natural gas as possible fuels with effectively low CO_2 footprint. However, in the proximity of liquids and liquid alcohols, large abundances of DME may be present if the corresponding methyl alcohol is in the basic liquid. This is consequently of great interest for applications of plasmas close to the boundary of the liquids such as in applications of atmospheric pressure plasmas in medicine [49–52], agriculture [53–55] and in sterilization of the resistant pathogens [56]. DME has been the subject of numerous studies for quite some time but nowadays one can expect better founded efforts as the field of applications is broadened and one may expect a wide range of ideas and advances.

The cross sections proposed by Biagi [16] were the basis of our work, and only limited changes were made in order to fit the whole range of the available transport data, especially the rates of ionization. However, cross sections of Biagi have an advantage of including the first order corrections for the anisotropy in scattering (through two moments of the cross section). It is our experience that for the lower mean energies where drift velocities may be measured, isotropic representation through the momentum transfer cross section usually works well enough. On the other hand, isotropic model of scattering becomes inadequate for very high

local E/N and for the mean energies above several eV [57, 58].

Author contribution

Iterative calculations required to fit the cross sections were performed by Snježana Dupljanin. All other calculations, verification of results, strategic planning, interpretations, preparation of the manuscript and projections of the impact on possible applications were completed with equal contributions of all coauthors.

Data Availability Statement This manuscript has no associated data or the data will not be deposited. [Authors' comment: Any reasonable request for numerical data will be responded to. In addition, data will soon be deposited in the LxCat and Quantemol data bases and in our group's data base.]

References

1. Z. Peeters, S. Rodgers, S.B. Charnley, L. Schriver-Mazzuoli, A. Schriver, J.V. Keane, P. Ehrenfreund, Astronom. Astrophys. **445**, 197 (2006)
2. R. Verbeek, J. van der Weide, SAE Technical Paper, 971607 (1997)
3. G. Mittal, M. Chaos, C.J. Sung, F.L. Dryer, Fuel Process. Technol. **89**, 1244 (2008)
4. M. H. J. Geijsberts, F. G. Hartjes, J. G. Pannekoek, J. Schmitz, F. Udo, *NIKHEF-H/91–21*
5. J. Miyamoto, I.P.J. Shipsey, Nucl. Phys. B (Proc. Supl.) **78**, 695–702 (1991)
6. F. Angelini, R. Bellazzini, A. Brez, M.M. Massai, G. Spandre, M.R. Torquati, Nucl. Instr. Meth. Phys. Res. A **283**, 755 (1989)

7. F. Sauli, Nucl. Instr. Meth. Phys. Res. A **386**, 531 (1997)

8. Y. Takeuchu, T. Tamagawa, F. Asami, A. Yoshikawa, T. Iwahasani, S. Konami, W. Iwakiri, J. Instrum. **7**, C03042 (2012)

9. Y. Takeuchu, T. Tamagawa, T. Kitaguchi, S. Yamada, W. Iwakiri, F. Asami, A. Yoshikawa, K. Kaneko, T. Enoto, A. Hayato, T. Kohmura, the GEMS/XACT team, J. Instrum. **9**, C01002 (2014)

10. T.L. Cottrell, I.C. Walker, Trans. Faraday Soc. **61**, 1585–1593 (1965)

11. F. Villa, Nucl. Instr. Meth. **217**, 273–276 (1983)

12. V. Cindro, H. Kolanoski, A. Lange, D. Lauterjung, F. Müller, T. Siegmund, W. Söder, H. Thurn, Nucl. Instr. Meth. Phys. Res. A **309**, 411–421 (1991)

13. E. Oettinger, M. Hilderbrandt, B. Schmidt, Nucl. Instr. Meth. Phys. Res. A **412**, 355–360 (1998)

14. T.L. Cottrell, I.C. Walker, Trans. Faraday Soc. **63**, 549–554 (1967)

15. A. Sharma, F. Sauli, Nucl. Instr. Meth. Phys. Res A **323**, 280–283 (1992)

16. S. Biagi, MAGBOLTZ (source file for version 10.0.2) http://magboltz.web.cern.ch/magboltz/

17. Z. Lj Petrović, M. Šuvakov, Ž Nikitović, S. Dujko, O. Šašić, J. Jovanović, G. Malović, V. Stojanović, Plasma Sources Sci. Technol. **16**, S1 (2007)

18. Z. Lj Petrović, S. Dujko, D. Marić, G. Malović, Ž Nikitović, O. Šašić, J. Jovanović, V. Stojanović, M. Radmilović-Rađenović, J. Phys. D Appl. Phys. **42**(19), 194002 (2009)

19. J.L. Pack, R.E. Voshall, A.V. Phelps, Phys. Rev. **127**, 2084 (1962)

20. L. G. H. Huxley, R. W. Crompton in *The Diffusion and Drift of Electrons in Gases* (New York: Wiley-Interscience, 1974)

21. S. R. Hunter, L. G. Christophorou in *Electron Molecule Interactions and their Applications*, vol **2**, edited by L G Christophorou (New York: Academic, 1984)

22. W.L. Morgan, Adv. At. Mol. Opt. Phys. **43**, 79 (2000)

23. M. Hayashi, Compilation of electron cross sections, LXcat database, http://www.lxcat.net

24. W. L. Morgan, Compilation of electron cross sections used by Kinema Research & Software, LXcat database, http://www.lxcat.net

25. W.L. Morgan, B.M. Penetrante, Comp. Phys. Commun. **58**, 127 (1990)

26. Z.M. Raspopović, S. Sakadžić, S. Bzenić, Z. Lj Petrović, IEEE Trans. Plasma Sci. **27**, 1241 (1999)

27. R.D. White, R.E. Robson, B. Schmidt, M.A. Morrison, J. Phys. D Appl. Phys. **36**, 3125 (2003)

28. S.A. Lawton, A.V. Phelps, J. Chem. Phys. **69**, 1055–1068 (1978)

29. K. Tachibana, A.V. Phelps, J. Chem. Phys. **71**, 3544 (1979)

30. M. Kurihara, Z. Lj Petrović, T. Makabe, J. Phys. D Appl. Phys. **33**(17), 2146 (2000)

31. A. Okigawa, M. Tadokoro, A. Itoh, N. Nakano, Z. Lj Petrović, T. Makabe, Jpn J Appl Phys **36**(7S), 4605 (1997)

32. M. Tadokoro, A. Itoh, N. Nakano, Z. Lj Petrović, T. Makabe, Phys. Rev. E **57**(1), R43 (1998)

33. S. Dujko, R.D. White, K.F. Ness, Z. Lj Petrović, R.E. Robson, J. Phys. D Appl. Phys. **39**, 4788 (2006)

34. Z. Lj Petrović, Z.M. Raspopović, S. Dujko, T. Makabe, Appl. Surf. Sci. **192**, 1–25 (2002)

35. R.D. White, K.F. Ness, R.E. Robson, Appl. Surf. Sci. **192**, 26–49 (2002)

36. R.D. White, S. Dujko, K.F. Ness, R.E. Robson, Z.M. Raspopović, Z. Lj Petrović, J. Phys. D Appl. Phys. **41**, 025206 (2008)

37. S. Bzenić, Z. Lj Petrović, Z.M. Raspopović, T. Makabe, Jpn. J. Appl. Phys. **38**, 6077 (1999)

38. Z.M. Raspopović, S. Dujko, T. Makabe, Z. Lj Petrović, Plasma Sources Sci. Technol. **14**, 293–300 (2005)

39. R.D. White, R.E. Robson, K.F. Ness, Aust. J. Phys. **48**, 925 (1995)

40. K. Maeda, T. Makabe, N. Nakano, S. Bzenić, Z. Lj Petrović, Phys. Rev. E **55**, 5901 (1997)

41. S. Dupljanin, O. Šašić and Z. Lj. Petrović in *Contributed Papers and Abstracts of Invited Lectures, Topical Invite Lectures and Progress Reports of the 27th Symposium on Physics of Ionized Gases – SPIG, Belgrade, Serbia*, 2014, edited by D. Marić, A. R. Milosavljević, Z. Mijatović, P1.32, pp 146–149

42. O. Šašić, S. Dupljanin, Z. Lj. Petrović *in ICOPS 2015 Abstract Book, The 42nd IEEE International Conference On Plasma Science,Belek, Antalya, Turkey,*2015

43. S. Dupljanin , O. Šašić, Z. Lj. Petrović *in Book of Abstracts of POSMOL 2019, XX International Workshop on Low—Energy Positron and Positronium Physics, XXI International Symposium on Electron—Molecule Collisions and Swarms*, Belgrade, Serbia, 2019, (Eds. D. Cassidy, M. J. Brunger, Z. Lj. Petrović, S. Dujko, B. P. Marinković, D. Marić, S. Tošić), 127.

44. M.J.E. Casey, P.W. Stokes, D.G. Cocks, D. Bošnjaković, I. Simonović, M.J. Brunger, S. Dujko, Z. LjPetrović, R.E. Robson, R.D. White, Plasma Sources Sci. Technol. **30**, 035017 (2021)

45. T. Makabe, Z. Lj Petrović, *Plasma electronics: applications in microelectronic device fabrication* (Taylor and Francis, New York, 2016)

46. D. Bošnjaković, Z. Lj Petrović, S. Dujko, J. Phys. D Appl. Phys. **49**, 405201 (2016)

47. S. Dujko, D. Bošnjaković, I. Simonović, Z. Lj. Petrović, R. D. White, *in Book of contributed papers, SAPP XXII, 22nd Symposium on Application of Plasma Processes and 11th EU-Japan Joint Symposium on Plasma Processing,* Štrbske Pleso, Slovakia, 2019 (Edited by V. Medvecka, J. Orszagh, P. Papp and Š. Matejčik), p. 57

48. D. Bošnjaković, Z. Lj Petrović, S. Dujko, J. Instrum. **9**, P09012 (2014)

49. L. Vialetto, P. Viegas, S. Longo, P. Diomede, Plasma Sources Sci. Technol. **29**, 115006 (2020)

50. Th. von Woedtke, S. Reuter, K. Masur, K.-D. Weltmann, Phys. Rep. **530**, 291 (2013)

51. R.E. Sladek, E. Stoffels, J. Phys. D Appl. Phys. **38**, 1716 (2005)

52. M.G. Kong, G. Kroesen, G. Morfill, T. Nosenko, T. Shmizu, J. van Dijk, J.L. Zimmermann, New J. Phys. **11**, 115012 (2009)

53. N. Puač, M. Gherardi, M. Shiratani, Plasma Process. Polym. **15**, 1700174 (2018)

54. C. Bradu, K. Kutasi, M. Magureanu, N. Puač, S. Živković, J. Phys. D Appl. Phys. **53**, 223001 (2020)

55. S. Živković, N. Puač, Z. Giba, D. Grubišić, Z. Lj Petrović, Seed Sci. Technol. **32**(3), 693–701 (2004)
56. J. Ehlbeck, U. Schnabel, M. Polak, J. Winter, Th. von Woedtke, R. Brandenburg, T. von dem Hagen, K.D. Weltman, J. Phys. D Appl. Phys. **44**, 13002 (2011)
57. V.D. Stojanović, Z. Lj Petrović, J. Phys. D **31**, 834 (1998)
58. S. Dujko, D. Bošnjaković, Z. Lj. Petrović and T. Makabe, in preparation.